Mitigation of the Torque Ripple of a Switched Reluctance Motor Through a Multiobjective Optimization

S. I. Nabeta[1], I. E. Chabu[1], L. Lebensztajn[1], D. A. P. Corrêa[2], W. M. da Silva[2], and K. Hameyer[3]

[1]Laboratório de Eletromagnetismo Aplicado do Departamento de Engenharia de Energia e Automação Elétricas, Escola Politécnica da Universidade de São Paulo (LMAG/PEA/EPUSP), São Paulo, Brasil

[2]CTM-SP Centro Tecnológico da Marinha

[3]IEM-Institut für Elektrische Maschinen RWTH Aachen, Aachen, Germany

The purpose of this work is to perform a multiobjective optimization in a 4:2 switched reluctance motor aiming both to maximize the mitigation of the torque ripple and to minimize the degradations of the starting and mean torques. To accomplish this task the Pareto Archived Evolution Strategy was implemented jointly with the Kriging Method, which acts as a surrogate function. The technique was applied on the optimization of some rotor geometrical parameters with the aid of finite element simulations to evaluate the approximation points for the Kriging model. The numerical results were compared to those from tests.

***Index Terms*—Electrical machines, finite element method (FEM), Kriging method, multiobjective optimization.**

I. Introduction

DUE TO its intrinsic geometrical characteristics, switched reluctance motors (SRMs) produce greater torque ripple when compared to traditional rotating motors. Such torque ripple is very troublesome because it generates vibration and audible noise [1]. Unfortunately, in most cases, the mitigation of the torque ripple implies in the degradation of other important features, such as the starting and the mean torques. To deal with this antagonism multiobjective optimization techniques seem to be the most suitable approach.

This paper proposes the combination of a multiobjective technique with the finite element method (FEM) for the optimization of some geometrical rotor parameters of a 4:2 SRM. This optimization will consider the mitigation of the torque ripple as well as the minimal degradations of the starting and mean torques.

The multiobjective optimization approach is based on the use of the Pareto Archived Evolution Strategy (PAES) jointly with the Kriging Method, which replaces the surrogate function as objective-function.

The finite element simulations provided the static torque values within a pole pitch as approximation points for the Kriging model.

The optimized rotor was prototyped and the SRM was submitted to tests in order to verify the proposed features.

II. Switched Reluctance Motor

The SRM considered in this work presents some unusual geometrical characteristics such as asymmetrical poles and a nonconstant air-gap. This new design was conceived in order to improve the starting unidirectional torque in any rotor position [2]. Despite the advantages achieved by such design the SRM presents an intrinsic nonnegligible torque ripple, which produces vibration and audible noise.

Fig. 1 depicts the main geometrical characteristics of the SRM and the details of the rotor.

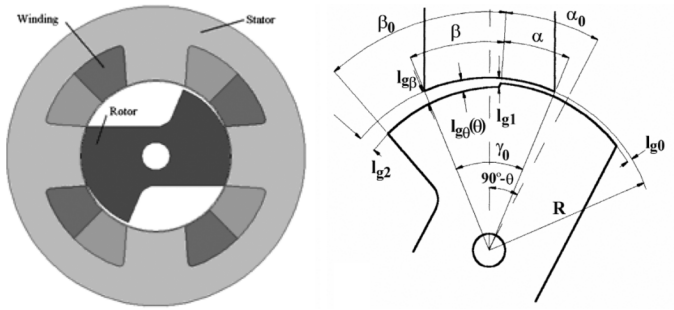

Fig. 1. SRM geometric characteristics and details of the rotor.

TABLE I
Geometric Characteristics of the SRM

Characteristic	Value
Stator outer diameter	90 mm
Stator yoke thickness	10 mm
Rotor diameter	2R = 45 mm
Core length	L_c = 35 mm
Stator pole arc	$\gamma_0 = 45°$
Rotor pole arc	$2\alpha_0 = 45°$
Main air-gap thickness	l_{g0} = 0.3 mm

The general geometric characteristics of this SRM are summarized in Table I.

III. Multiobjective Optimization

As stated formerly, the main goal of the multiobjective optimization was to minimize the torque ripple taking into account a minimal degradation of the mean and starting torques. Based on previous analytical evaluations of sensibility, three rotor parameters were chosen, namely β_0, l_{g1} and l_{g2}, for the optimization procedure. Thus the task was to find the best combination of values for β_0, l_{g1} and l_{g2} to accomplish the task.

The first objective-function is associated to torque ripple, and it is presented in (1), where $\bar{C}$ is the mean torque as defined in (2), $C(\theta)$ is the static torque at angular position θ, and $C(\theta_0)$ is the starting torque. In order to favor the starting torque $C(\theta_0)$ it has a different contribution to the value of the objective function.

Digital Object Identifier 10.1109/TMAG.2007.915137

TABLE II
PARAMETERS VARIATION DOMAIN

Parameter	Reference Value	Minimum Value	Maximum Value
β_0	45°	30°	60°
l_{g1}	0.6 mm	0.4 mm	0.6 mm
l_{g2}	1.2 mm	0.6 mm	1.8 mm

The second objective function is the mean torque as presented in the following:

$$f(\beta_0, l_{g1}, l_{g2}) = (\bar{C} - C(\theta_0)) + \sum_{i=1}^{n} |C(\theta_i) - \bar{C}| \quad (1)$$

$$\bar{C} = \frac{1}{\theta_n} \sum_{i=0}^{n-1} \frac{|C(\theta_{i+1}) - C(\theta_i)|}{2} (\theta_{i+1} - \theta_i). \quad (2)$$

For every triple $(\beta_0, l_{g1}, l_{g2})$ and for θ ranging within one pole pitch, 2-D nonlinear magnetostatic FEM simulations were carried out to obtain the torque values to be used in (1). The triple was equally distributed on a grid $(5 \times 5 \times 5)$ which resulted in 125 FEM calculations for the analysis. The variation domain for each parameter to be optimized is presented in Table II.

A multiobjective optimization problem is: the minimization of the torque ripple as defined by (1) and the maximization of the mean torque as presented in (2).

The adopted multiobjective algorithm was PAES [3], and a Kriging approach [4] was used to build the surrogate functions.

IV. KRIGING METHOD

A. Qualitative Approach

Kriging exploits the spatial correlation of data in order to build interpolations and uses the realization of a stochastic process to model the interpolation. The method will firstly be presented as an intuitive approach, as proposed in [4].

The method could be understood as follows: the goal is to interpolate a set of N samples and the interpolation function is defined with two classes of functions: the first describes the general trend, e.g., it will follow the general tendency of the function to be modeled. It is generally a constant, although some works adopt a polynomial function of order 2. The other class of function will locally describe the data, e.g., it shows the behavior of the fluctuations around the general trend and it is usually built with a set of Gaussians.

Fig. 2 shows how Kriging works. The function was interpolated by two kinds of functions: the first one is a constant trend. The second set of functions is the fluctuations: they describe locally the function around the trend.

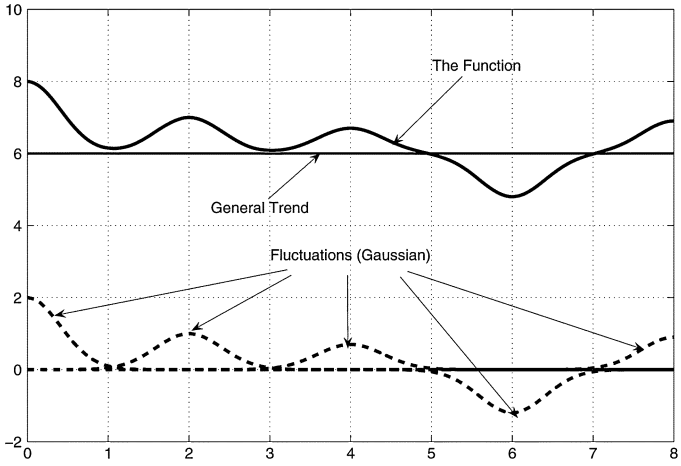

Fig. 2. Kriging approach.

B. Formulation

In this work, we will formulate Kriging using the Design and Analysis of Computer Experiments (DACE) approach. DACE uses maximum-likelihood estimates (MLEs) to build Kriging interpolations. First of all, a Kriging model could be defined as follows:

$$y(\mathbf{x}) = f(\mathbf{x}) + Z(\mathbf{x}) \quad (3)$$

where $\mathbf{x}$ is the optimization vector $[x^1\ x^2 \cdots x^{\mathrm{Npar}}]^T$; N_{par} is the number of design variables; x^k is the kth design variable of the optimization vector $\mathbf{x}$; $y(\mathbf{x})$ is the interpolation function, $f(\mathbf{x})$ is a global model (adopted constant and equals to β) and $Z(\mathbf{x})$ is the realization of a random process $N(0, \sigma^2)$ with a nonzero covariance.

The definition of a Kriging model as stated by (3) follows the qualitative description: the global model $f(\mathbf{x})$ is a trend, and $Z(\mathbf{x})$ is a realization of a random process is a set of local departures (the Gaussian functions). Now, the mathematical problem is to find the best values of β and σ^2 for data interpolation. In order to solve this problem, the covariance matrix of $Z(x)$ is defined

$$\mathrm{Cov}[Z(y(\mathbf{x}_i)), Z(y(\mathbf{x}_j))] = \sigma^2 R(\mathbf{x}_i, \mathbf{x}_j). \quad (4)$$

The correlation matrix is $\mathbf{R}$ with a generic element defined by the correlation function $R(x_i, x_j)$

$$R(x_i, x_j) = \exp[-\theta \|\mathbf{x_i} - \mathbf{x_j}\|^2] \quad (5)$$

where $\|.\|$ is a ℓ^2 norm and the θ is a positive constant, which measures how the data are correlated.

The best linear unbiased predictor (BLUP) of $y(x)$ is

$$y^*(x) = \beta(\theta) + \mathbf{r^T}(x, \theta)\mathbf{R}(\theta)^{-1}(\mathbf{y} - \mathbf{f}\beta(\theta)) \quad (6)$$

where $y^*(x)$ is the estimated value at x, $\mathbf{y}$ is a $N \times 1$ vector filled with the sampled values, $\mathbf{f}$ is a $N \times 1$ vector filled by ones, because the trend was assumed constant. Vector $\mathbf{r^T}(x)$ is the correlation vector between x and the N sample points, e.g.,

$$\mathbf{r^T}(\mathbf{x}) = [R(\mathbf{x}, \mathbf{x}_1) \quad R(\mathbf{x}, \mathbf{x}_2) \quad \cdots\cdots \quad R(\mathbf{x}, \mathbf{x}_N)]^T. \quad (7)$$

Given the value of θ, the $\hat{\beta}$ and $\hat{\sigma}$ could be estimated as

$$\hat{\beta}(\theta) = (\mathbf{f^T}\mathbf{R}(\theta)^{-1}\mathbf{f})^{-1}(\mathbf{f^T}\mathbf{R}(\theta)^{-1}\mathbf{y}) \quad (8)$$

$$\hat{\sigma}^2(\theta) = [(\mathbf{y} - \mathbf{f}\beta(\theta))^T\mathbf{R}(\theta)^{-1}(\mathbf{y} - \mathbf{f}\beta(\theta)]/N \quad (9)$$

and the MLE of θ could be obtained by maximizing

$$-(N(\ln(\hat{\sigma}^2(\theta)) + \ln(\det(\mathbf{R}(\theta))))/2. \quad (10)$$

The solution of (10) gives the value of θ and (6) allows to evaluate the function for any value of x.

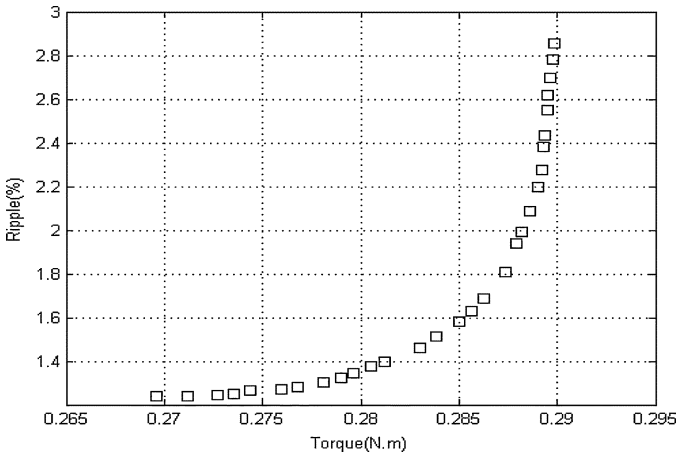

Fig. 3. Pareto set.

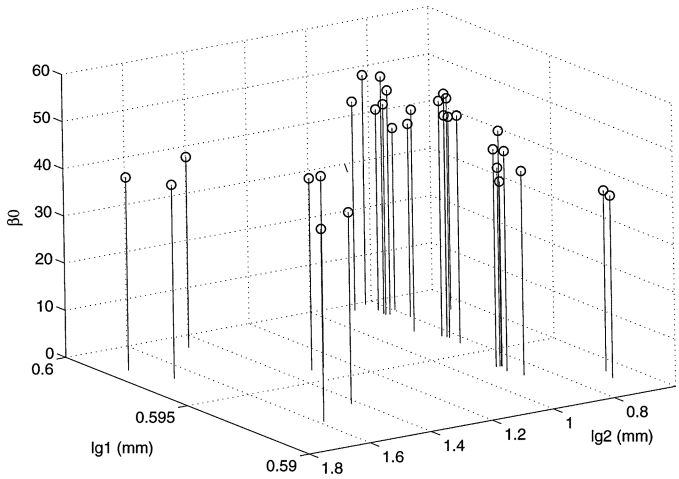

Fig. 4. Nondominated solutions.

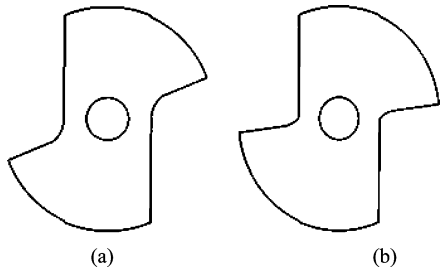

Fig. 5. Rotor geometry. (a) Before optimization. (b) After optimization.

V. Pareto Archived Evolution Strategy

The Pareto Archived Evolution Strategy (PAES) is a multiobjective optimizer that applies a local search evolution strategy. In order to well understand PAES, a pseudocode for $(1 + 1)$ PAES as proposed in [3] is presented. It is subdivided in three parts: the candidate solution generator, the acceptance function and the Non-Dominated Solutions (NDS) archive management.

i) Generate initial random solution c and add it to the archive
ii) Mutate c to produce m and evaluate m
iii) if (c dominates m) $\{\text{discard } m\}$
iv) else if (m dominates c) $\{$ replace c with m and add m to the NDS archive $\}$
v) else if (m is dominated by any member of the archive) $\{\text{discard } m\}$
vi) else apply *test* (c, m, archive) to determine which becomes the new current solution and whether to add m to the NDS archive
vii) until a termination criterion has been reached return to line ii)

The pseudocode shows that the acceptance function and the NDS archive work together. A new candidate solution fm could only enter into the archive when m is not dominated by c. Nevertheless, it could be discarded when any member of the archive dominates m. The great problem appears when there is no dominance between m and c. In this case, the procedure called *test*(c, m archive) will define the new current solution and identify the conditions when m will be added to the NDS archive. For example, when the archive is not full, m could always be accepted. In other hand, if the archive is full and m is placed in a less crowded region than c, then c is discarded of the NDS archive, m will enter in the NDS archive and m replaces c as the current solution.

VI. Results

A. Multiobjective Optimization

The multiobjective optimization provided the Pareto set as depicted in Fig. 3. The prototype was constructed with the following values: $\beta_0 = 50°, l_{g1} = 0.6$ mm and $l_{g2} = 0.8$ mm.

After obtaining a Pareto-set it is always important to analyze the sensitivity of the set with respect to the optimization parameters. Fig. 4 shows the nondominated solutions on the design variable space. A qualitative approach allows us to observe that the variance of the parameter l_{g1} is extremely low, and the value of l_{g1} should be closer to its upper bound to improve the mean torque and to minimize the torque ripple. The torque ripple and the mean torque are highly dependent on l_{g2} and β_0. The parameter l_{g2} assumes values in the interval [0.75 1.8] and β_0 in the interval [37° 50°].

Fig. 5 shows the geometries for the original and the optimized rotors. Afterward, two prototypes were constructed and tests were carried out in order to validate the numerical results.

B. Tests

To validate the numerical results the static torque measurement was firstly obtained. It was carried out within a range of [$-20°$ to 90°] for θ as presented in Fig. 6.

From Fig. 6 one can note that the starting torque at $\theta = 0°$ is twice larger in the optimized prototype. The mean torque, calculated in the range of 0° to 90°, the starting torque and the torque ripple are summarized in Table III.

For dynamic operation one can consider that the subsequent phase is switched nearly at $\theta = 90°$. Thus, even though the optimized prototype presents a sag in the torque curve, it is still capable of driving heavier loads because its minimum torque in the 0° to 90° region is higher than the original design. Also, the torque ripple, considered as the difference between the maximum and the minimum values in the 0° to 90° region, has reduced while its frequency has doubled. This last characteristic provides a better mechanical stability for the driven load

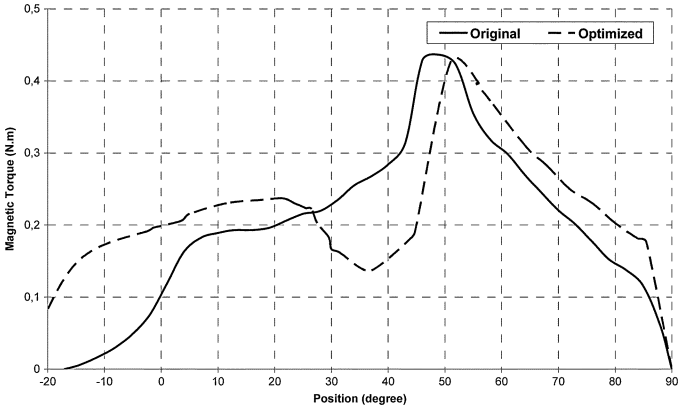

Fig. 6. Static torque measurements for both prototypes.

TABLE III
TORQUE CHARACTERISTICS

	Original Prototype	Optimized Prototype
Mean Torque (N.m)	0.23	0.24
Starting Torque (N.m)	0.10	0.20
Torque Ripple (N.m)	0.34	0.23

because its inertia softens the ripple effects at the double the frequency.

Moreover, the optimized prototype presents higher torques in the region $60° < \theta < 90°$. It allows the electronic drive to switch in a broader range rendering the motor operation more flexible.

The torque ripple was also measured indirectly through the vibration-signal acquisition followed by a fast Fourier transform (FFT) analysis. The SRM was tested at the nominal speed and torque, 6000 rpm (100 Hz) and 0.28 Nm, respectively.

As the torque ripple measurement in dynamic operation is unfeasible, the vibration was measured instead. The torque ripple introduces torsional rotor pulsations, which induces vibration in the motor frame at ripple frequency. So, the induced vibration on motor structure is an indirect measurement of the effect of torque ripple.

A piezoelectric accelerometer was used for the vibration measurement.

Due to the four stator poles, the main component of the torque ripple frequency at nominal speed is four times higher, i.e., 400 Hz. Thus the vibration-signal acquisition was followed by a FFT analysis in the vicinity of 400 Hz as shown in Fig. 7.

VII. CONCLUSION

A numerical multiobjective optimization procedure was proposed by using finite element simulations, the Kriging model and the Pareto Archived Evolution Strategy. The procedure was applied on the improvement of torque characteristics of a 4:2 SRM and new rotor geometry was obtained.

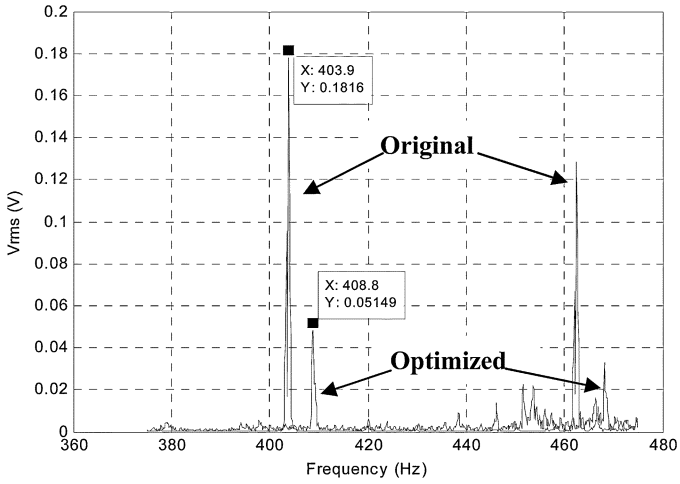

Fig. 7. Vibration analysis.

The optimized prototype was constructed and tested and confirmed the goals of the multiobjective optimization, i.e., a higher starting torque, a slightly higher mean torque and a lower ripple rate.

Considering the original design as the reference and analyzing only the static torque curves, the optimized prototype presented a starting torque 25% bigger and a torque ripple 57.6% smaller. From the dynamic test at rated speed and load, it was observed a significant reduction (71.65%) of the vibration in the vicinity of 400 Hz, which corroborates to validate the proposed procedure.

ACKNOWLEDGMENT

This research was supported by CAPES (PROBRAL-218/05).

REFERENCES

[1] B. Schmülling, K. Kasper, and K. Hameyer, "Acoustic optimization of a switched reluctance machine using numerical simulation," in *Proc. ICEM2006 Int. Conf. Electrical Machines*.

[2] I. E. Chabu, S. I. Nabeta, and J. R. Cardoso, "Design aspects of 4:2 pole-2 phase switched reluctance motors," in *Proc. IEEE IEMDC*, 1999, vol. 1, pp. 63–65.

[3] J. D. Knowles and D. Corne, "Approximating the nondominated front using the pareto archived evolution strategy," *Evolut. Comput.*, vol. 8, no. 2, pp. 149–172, 2000.

[4] L. Lebensztajn *et al.*, "Kriging: A useful tool to electromagnetic devices optimization," *IEEE Trans. Magn.*, vol. 40, no. 2, pp. 1196–1199, 2004.

Manuscript received June 24, 2007. Corresponding author: S. I. Nabeta (e-mail: nabeta@pea.usp.br).